Chiari I Malformations: Assessment with Phase-Contrast Velocity MR

Samuel M. Wolpert, Rafeeque A. Bhadelia, Andrew R. Bogdan, and Alan R. Cohen

PURPOSE: To assess movement of the medulla, tonsils, and upper cervical cord as well as that of the posterior fossa cerebrospinal fluid pathways in both normal subjects and those with Chiari I malformations. **METHODS:** Nine healthy volunteers and eight patients with Chiari I malformations were examined with phase-contrast cine MR. With a region-of-interest cursor, the directions and intensities of the brain and cerebrospinal fluid were assessed and intensity-versus-time graphs generated. **RESULTS:** Cerebrospinal fluid flow patterns of the patients with Chiari I malformations were normal except for absence of valleculla flow. In addition, increased velocities (10 times normal) of the tonsils of all patients with Chiari I malformations together with posterior movement of the medulla (rather than the expected anterior movement seen in volunteers) occurred. **CONCLUSIONS:** Increased velocities of the tonsils may be the result of the carotid systolic pulse being delivered to a structure (the tonsil) without the normal surrounding cerebrospinal fluid, resulting in impact of the tonsils in the confined foramen magnum and a consequent caudocranial recoil. An alternative explanation would include the Bernoulli effect caused by the confined location of the tonsils. There may be a decrease in the peak tonsillar velocities after surgery.

Index terms: Chiari malformation; Cerebrospinal fluid, flow dynamics; Neck, magnetic resonance; Spine, magnetic resonance; Magnetic resonance, flow studies

AJNR Am J Neuroradiol 15:1299–1308, Aug 1994

Patients with Chiari I malformations who are symptomatic because of crowding of the posterior fossa structures at the foramen magnum may benefit from suboccipital craniectomy and upper cervical laminectomy (1). If the patients are symptomatic because of cerebrospinal fluid (CSF) flow obstruction or impedance, a noninvasive test to examine the flow at the foramen magnum and possibly to assess disease severity and the benefits of surgery may be of help. Magnetic resonance (MR) is an excellent test for the evaluation of patients with the malformation; not only can the abnormality be easily diagnosed (2, 3), but CSF flow at the foramen magnum can be detected with phase-contrast flow-sensitive MR techniques (4).

Recently we began using flow-sensitive velocity MR techniques in the study of symptomatic patients with Chiari I malformations to determine the CSF flow dynamics at the foramen magnum. Concurrently, we also observed the brain motion of cerebral parenchymal structures (both velocity and direction changes) as has previously been described (5, 6). In the patients with Chiari I malformations, although only minor changes in CSF flow pattern were seen, unexpected large velocity increases were noted in the tonsils with accompanying abnormal movements of the medullae and upper spinal cords. An analysis of the CSF flow patterns and those of the tonsils, medullae, and upper cervical cords is the subject of this report.

Patients and Methods

This prospective study was performed with a 1.5-T imager (Signa, General Electric Medical Systems, Milwaukee, Wis, software version 5.2). Nine healthy subjects (six adults and three children) and eight patients (five adults and three children) were examined. The healthy adults were volunteers, and the healthy children were patients

Received July 27, 1993; accepted pending revision September 22; revision received October 20.

Presented at the 31st Annual Meeting of ASNR, Vancouver, Canada, May 16–20, 1993.

From the Section of Neuroradiology, Department of Radiology (S.M.W., R.B., A.B.) and the Departments of Medical Physics (A.B.) and Neurosurgery (A.C.), New England Medical Center Hospitals, Boston.

Address reprint requests to Samuel M. Wolpert, MD, New England Medical Center Hospitals, 750 Washington St, Boston, MA 02111.

AJNR 15:1299–1308, Aug 1994 0195-6108/94/1507–1299

undergoing flow studies to differentiate large cisterna magnae from retrocerebellar arachnoid cysts. (All three children were subsequently diagnosed as having large but normal cisterna magnae.)

The eight patients ranged in age from 6 to 24 years and presented with headaches of varying severity (n = 7), neck pain (n = 1), numbness or burning sensation in the hands (n = 1), and dizziness (n = 1). Some of the patients had multiple symptoms. Scoliosis and ataxia were the most frequently associated clinical signs (n = 4). Nystagmus and mild myelopathy each were present in single patients.

Six of the patients were studied before and two after surgery. The diagnosis of Chiari I malformations was made by visualizing pointed cerebellar tonsils extending below the plane of the foramen magnum. The tonsils were between 20 and 32 mm below in six patients and 12 and 10 mm below in two patients. Hydrosyringomyelia of the upper cord was present in three patients. Hydrocephalus was not present in any of the patients. Seven patients were treated with a suboccipital craniectomy and upper cervical laminectomy. One patient with mild headaches, a normal examination, and tonsils 25 mm below the plane of the foramen magnum is being followed up without surgery.

The study was carried out using a commercially available phase-contrast cine MR pulse sequence (7). The sequences and techniques used are based on those previously proposed by Enzmann and Pelc to assess brain motion (8) with some modifications. The scan thicknesses were 3 mm, and the studies were obtained in the midline sagittal projection. The pulse sequence was retrospectively gated, and the repetitions were executed continuously at a constant rate with consecutive phase-encoding amplitudes being incremented at the detection of the R wave from a peripheral pulse trigger (finger photoplethysmograph). The technical factors were: repetition time of 54; echo time 10; matrix 128 × 256; two signals averaged; field of view 24 cm; and flip angle 15°. The lowest available velocity encoding on the scanner, 5 cm/s, was used, and the acquired data were reconstructed to produce 16 frames in the cardiac cycle. In patients and volunteers with relatively rapid heart rates, fewer than 16 frames were acquired; in these subjects the data were interpolated to register 16 points in each cardiac cycle.

The intensities of the acquired signals of CSF and brain were assessed using a region-of-interest cursor and areas varying between 0.4 and 1.0 cm^2. Care was taken not to include blood vessels in the selected areas. The regions of interest included the CSF spaces around the upper cord, the prepontine cistern, the aqueduct, and the fourth ventricle. The aqueduct was measured at its junction with the fourth ventricle. It was impossible to avoid partial volume errors with this latter measurement. Regions of interest of the tonsils, medullae, and upper cervical cords were obtained (Fig 1). To decrease baseline errors caused by gradient-induced eddy currents, the averages of the signal intensities from all the regions of interest from a given area were subtracted from the intensities at each of the 16 points in the cardiac cycle, and the resultant intensity used

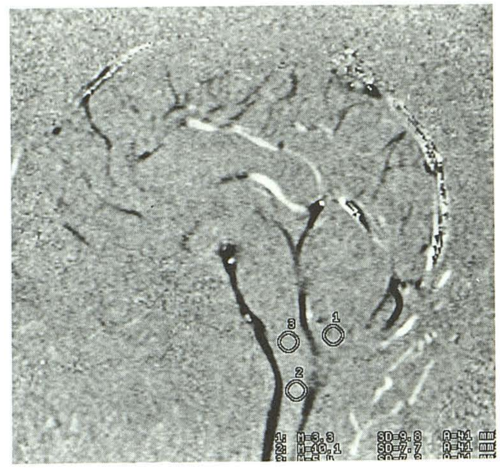

Fig 1. Sagittal velocity-encoded image obtained during CSF diastole demonstrates the three areas (*1*, tonsil; *2*, upper cord; and *3*, medulla) where regions of interest are obtained. Note the *dark signal* representing cephalad CSF flow around the upper cord and in the prepontine cistern, aqueduct, floor of the fourth ventricle, and vallecula.

in subsequent calculations as has been described previously (8).

All the subjects were assessed for motion encoding in the superior-inferior direction. With this technique a bright signal indicates velocity in the superior-inferior direction and a dark signal velocity in the inferior-superior direction. The brighter the signal the higher the velocity in the chosen direction; the darker the signal the higher the velocity in the opposite direction. No attempt was made to calculate the actual velocities of the structures studied because of the inherent inaccuracy in calculating flow velocities from weighted-phase images (see below). A relatively low velocity encoding of 5 cm/s was chosen to encompass both the slow velocity of the brain and the relatively rapid velocity of the CSF. Aliasing occasionally occurred in rapidly flowing CSF and was easily recognized by the abrupt change between high- and low-signal pixels in the center of the CSF compartments where the flow velocity was at a maximum. Care was taken not to include the areas of aliasing in the regions of interest.

In six of the volunteers (four adults and two children) and in six of the patients (four adults and two children) velocity-encoding studies of the tonsils, medullae, and upper cervical cords were also carried out in the anteroposterior direction. A bright signal indicated flow in the anteroposterior direction and a dark signal flow in the posteroanterior direction. To eliminate the possibility of partial volume measurements of the CSF surrounding the tonsils being incorporated in the regions of interest, flow studies in the axial plane with motion encoding in the superior-inferior direction were carried out in four healthy subjects and in six patients; in one patient superior-inferior encoding was obtained in the coronal plane. The regions of interest of the tonsils obtained in the axial and coronal

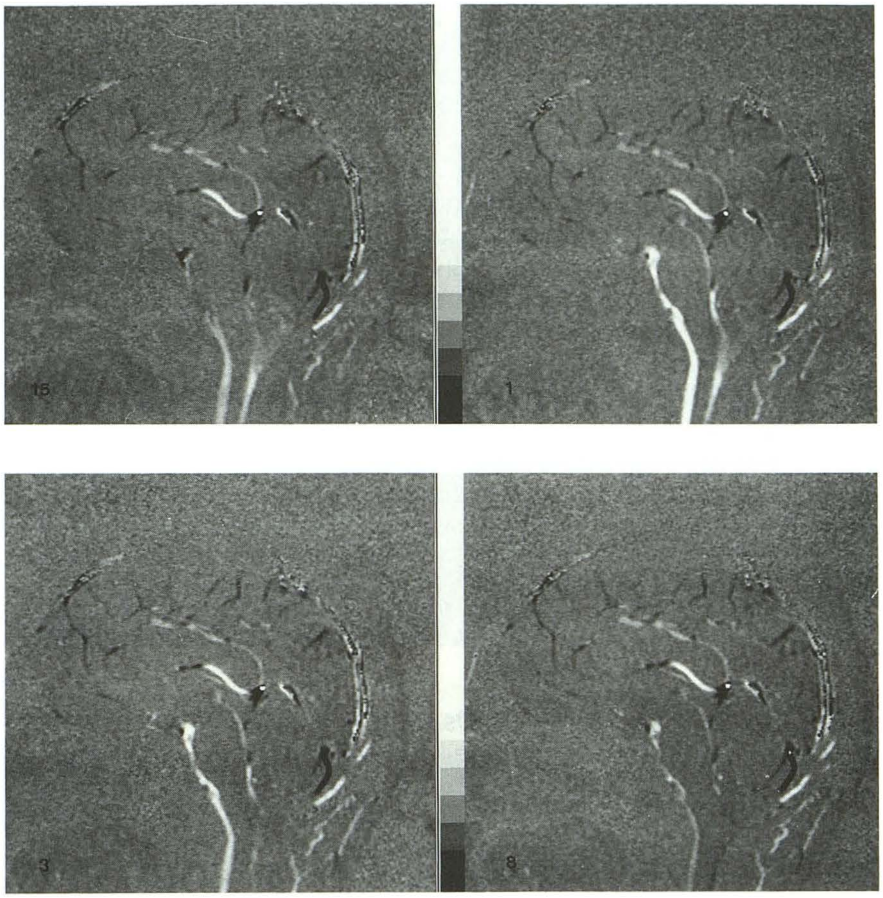

Fig 2. Series of four selected velocity-encoded images, superior-inferior encoding (images 15, 1, 3, and 8: *top left, top right, bottom left,* and *bottom right*) in a healthy subject. Note the caudal flow of CSF in the precord, postcord, and prepontine cisterns maximal on frames 1 to 3. Caudal flow of CSF is also seen in the aqueducts on frames 1, 3, and 8.

planes confirmed that the regions of interest accurately included the tonsils and not the surrounding CSF.

The region-of-interest analyses described in this paper were performed on the weighted-phase images. For each time point in the reconstruction of the cine phase-contrast data there are two images, a weighted-phase image and a magnitude image. The weighted-phase image is obtained by multiplying the phase information (in which pixel intensities are proportional to velocity) by the corresponding magnitude image. This creates an image more pleasing to the eye than a pure-phase image, but interpretation of the velocity of such an image may be suspect (see Addendum).

The motions of the CSF and the cerebral structures of the healthy subjects were compared with those of the patients with Chiari I malformations by summing the regions of interest at the same point of the cardiac cycle for all the volunteers and patients, obtaining the mean and standard deviation, and generating graphs of signal intensities versus frames of the cardiac cycles. The graphs were generated for flow in the superior-inferior and in the anteroposterior directions and the intensity values of the tonsils, medullae, and upper cords analyzed separately for the two directions using a split-plot analysis of variance with groups as the between-subjects factor and time (or frames of the cardiac cycle) as the repeated factor.

Results

Healthy Subjects

On the images, white (high signal intensity) represents caudal motion, and black (low signal intensity) represents cranial motion. The term *CSF systole* refers to caudal motion of the CSF, and the term *CSF diastole* refers to cranial motion of the CSF (8).

CSF Flow. CSF systole of the pericord CSF that commenced on frames 14 and 15 (Fig 2), was seen both behind and in front of the cords and in a few cases preceded a similar downward flow in the prepontine cisterns by one image. The caudal velocity was maximal on image 1.

Caudal CSF flow through the valleculae was almost synchronous or slightly delayed compared with pericord flow, and at the same time caudal flow was seen in the fourth ventricles. Caudal flow through the aqueducts commenced approximately two images (12%) later than the pericord flow and peaked at 12% to 20% through the cycle. There was no difference between the flow patterns of the children and the adults.

CSF diastole commenced between frames 2 and 7 (12% to 44% through the cycle) and was maximal between frames 8 and 13 at approximately 60% through the cycle (Fig 1). Diastolic CSF flow through the aqueducts began at 44%, peaked at 60% through the cycle, and lasted until commencement of the caudal flow in the pericord CSF.

Brain Parenchymal Movement. The tonsils, medullae, and upper cords were assessed for movement. With the selected lowest-available velocity encoding of 5 cm/s, the signal-to-noise ratios of the selected structures were lower than those of the CSF (as assessed by the standard deviation of the average of the regions of interest obtained at each point in the cardiac cycle). Nevertheless, although relatively noisy, a consistent pattern of movement was detected. Between frames 10 and 13 caudal movement of the tonsils occurred, followed immediately (one frame later) by a similar movement of the medullae and upper spinal cords. Posteroanterior movement of the tonsils, medullae, and upper spinal cords also occurred at approximately the same time as the tonsils and medullae moved inferiorly. There was no difference between the velocity and movement patterns of the children and the adults.

Patients with Chiari I Malformations

CSF Flow. It was difficult to distinguish systolic flow through the valleculae and the foramina of Magendie from the increased downward movement of the adjacent tonsils. CSF systole and diastole in the prepontine cisterns occurred at the same time in the cine cycles in the patients with Chiari I malformations as in the volunteers. However, in the patients with Chiari I malformations CSF diastolic flow in the precord CSF spaces preceded that in the volunteers by approximately 15% of the cine cycles. The CSF flow patterns through the aqueduct were normal (Fig 3).

Brain Parenchymal Movement. A consistent abnormal pattern of brain movement was seen at the foramina magna. In seven of the eight patients, the caudal and anterior velocities of the cerebellar tonsils were approximately 10 times those of the tonsils of the healthy subjects (Fig 3). In addition, the medullae moved posteriorly at the same time as the tonsils moved caudally and anteriorly. Increased caudal velocity of the upper cords was also seen. The increased caudal velocity of the tonsils was confirmed in the patients in whom axial and coronal acquisitions were obtained. The tonsillar velocity in one patient with mild headaches but tonsils 25 mm below the plane of the foramen magnum was also significantly increased. In all cases increased velocities of the tonsils, medullae, or upper cords in one direction were followed by similar increased velocities of these structures in the opposite direction. The tonsillar velocity in the patient with only mild headaches and tonsils 25 mm below the plane of the foramen magnum was also significantly increased. Figure 4 graphically demonstrates the increased velocities of the tonsils, upper cords, and medullae in the patients with Chiari I malformations compared with the healthy volunteers.

Discussion

In the 1890s Chiari described the postmortem findings in children with varying degrees of hindbrain deformity, with the type I malformation being characterized by cerebellar tonsil displacement through the foramen magnum with a normal position of the fourth ventricle (9). Radiologic techniques always have played a pivotal role in the diagnosis of the malformation (10) and have included iophendylate (Pantopaque) myelography and water-soluble myelography generally in conjunction with computed tomography. Currently MR is widely recognized as the procedure of choice. Tonsils may normally herniate up to 5 mm below the foramina magna in asymptomatic patients (11); generally tonsils below this level are necessary to diagnose the malformation. However, a large percentage (31%) of patients with tonsils herniating 5 mm or more below the foramina magna may be asymptomatic, with the herniation being discovered only when MR examinations are carried out for unrelated reasons (10). In the present study, in no patient were the tonsils less than 10 mm below the planes of the foramina magna.

Two recent studies described MR phase imaging to analyze the driving force of CSF (8, 12). Enzmann et al found an anterocaudal motion of the lower cerebellum and brain stem preceding a caudal motion of the diencephalon and upper brain stem (8). They also found that the caudal motion of the lower brain stem and

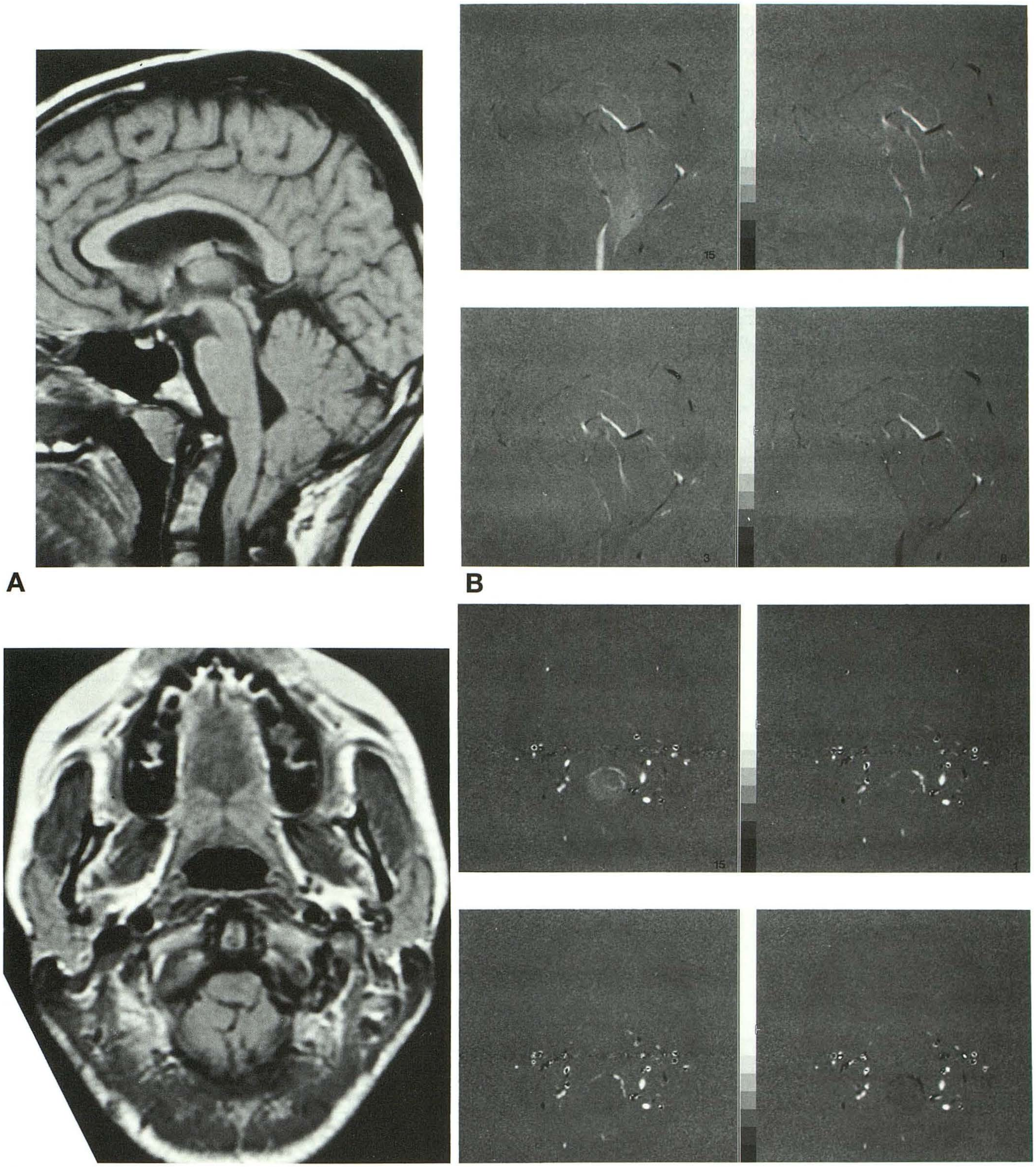

Fig 3. Patient with Chiari I malformation.

A, Sagittal T1-weighted image. Note the herniation of the tonsil through the foramen magnum.

B, Series of four selected velocity-encoded images, sagittal projection, superior-inferior encoding (images 15, 1, 3, and 8: *top left, top right, bottom left,* and *bottom right*). The CSF flow pattern is approximately identical to that of Fig 2. Note the hyperintensity (image 15) and the hypointensity (image 8) of the tonsil, indicating increased caudal and cranial velocities of the tonsil.

C, Axial T1-weighted image at the level of C-1 demonstrating the herniated tonsils.

D, Series of four selected velocity-encoded images, axial projection at the same level as *C,* superior-inferior encoding (images 15, 1, 3, and 8: *top left, top right, bottom left,* and *bottom right*). Note the hyperintensity (image 15) and the hypointensity (image 8) of the tonsil, indicating increased caudal and cranial velocities of the tonsil and confirming that the increased velocities are from the tonsils not the surrounding CSF.

Fig 4. *A* and *B*, Velocity graphs of normal and Chiari tonsils and medullae (all SI). The signal intensity (proportional to velocity) is shown on the vertical axis, and the 16 data points (labeled X_1 to X_{16}, representing frames of the cardiac cycle) are on the horizontal axis. The graphs represent the mean values of the intensities at the different points in the cardiac cycle. One-standard-deviation error bars are shown. All *P* values represent significance levels with analyses of variance. In the superior-inferior series, negative intensities represent caudal movement and positive intensities cranial movement.

A, Tonsils, superior-inferior encoding, healthy subjects versus patients with Chiari I malformations (F = 9.16; *df* = 1,15; *P* = .0001).

B, Medulla, superior-inferior encoding, healthy subjects versus patients with Chiari I malformations (F = 3.55; *df* = 1,15; *P* = .0001).

Note: SI indicates superior-inferior encoding.

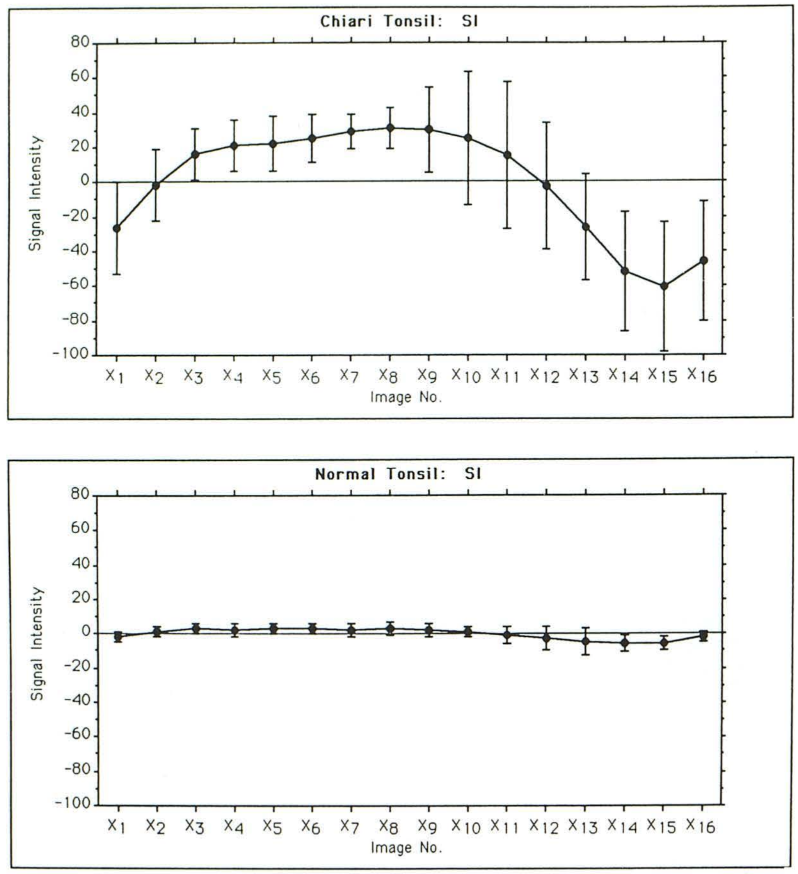

A

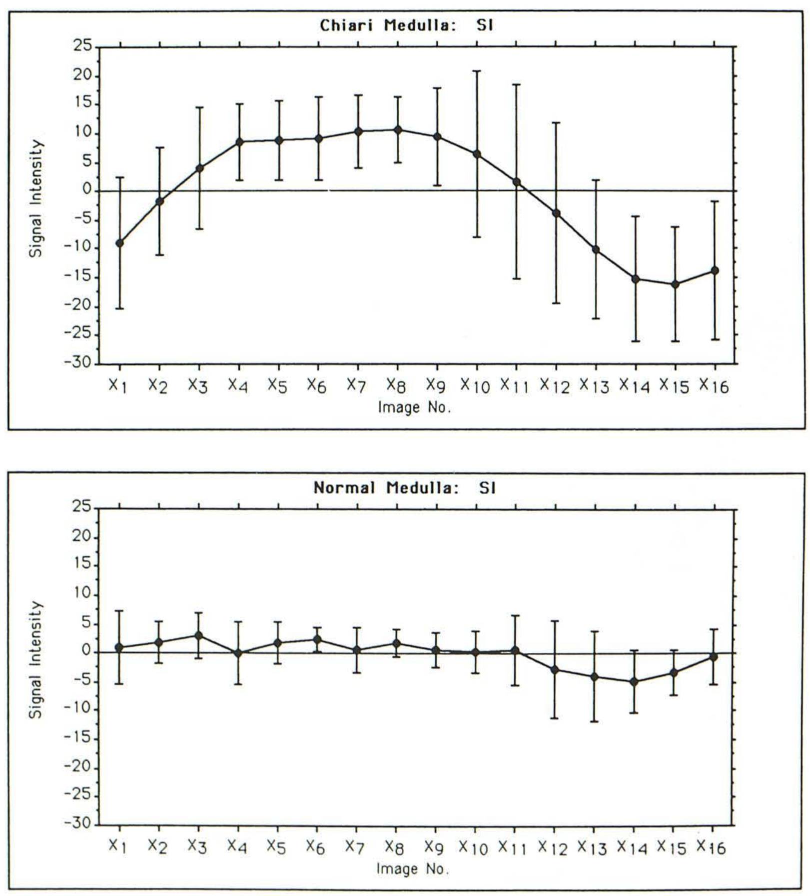

B

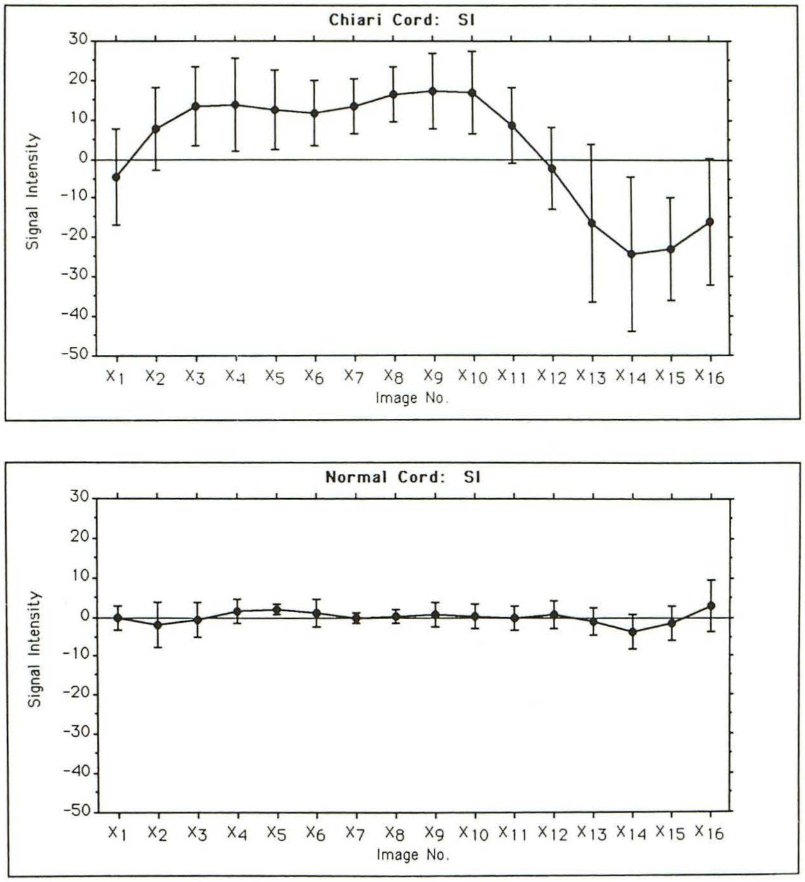

C

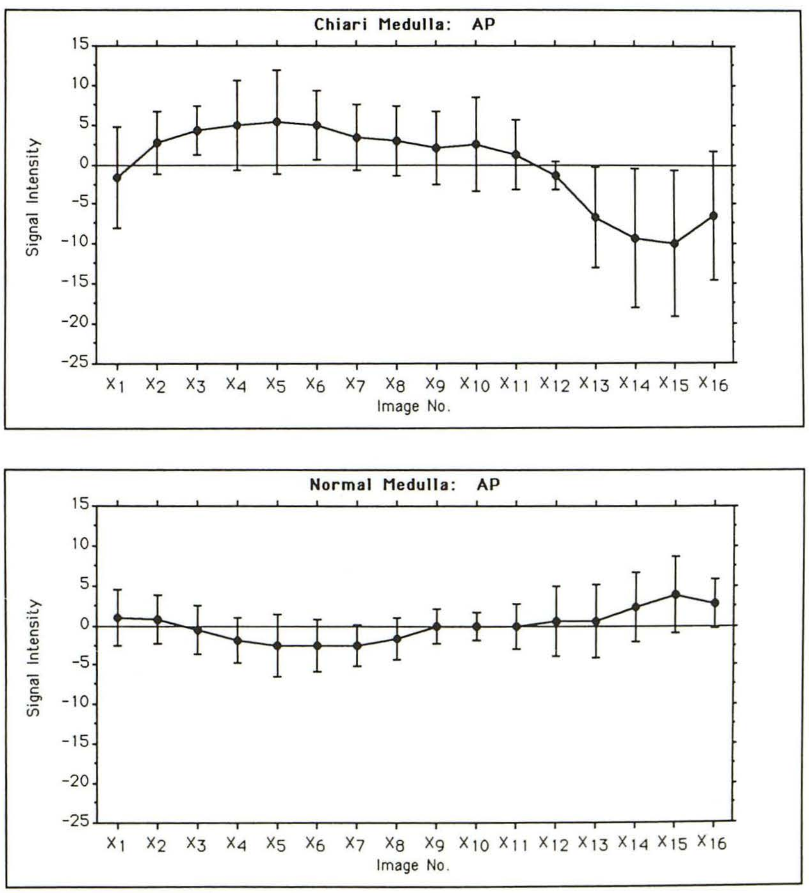

D

Fig 4. *C* and *D*, Velocity graphs of normal and Chiari upper cords (SI) and medullae (AP). The signal intensity (proportional to velocity) is shown on the vertical axis, and the 16 data points (labeled X_1 to X_{16}, representing frames of the cardiac cycle) are on the horizontal axis. The graphs represent the mean values of the intensities at the different points in the cardiac cycle. One-standard-deviation error bars are shown. All *P* values represent significance levels with analyses of variance. In the superior-inferior series, negative intensities represent caudal movement and positive intensities cranial movement. In the anteroposterior series, negative intensities represent anteroposterior movement and positive intensities posteroanterior movement.

C, Upper cord, superior-inferior encoding, healthy volunteers versus patients with Chiari I malformations (F = 7.56; df = 1,15; P = .0001).

D, Tonsils, anteroposterior encoding, healthy volunteers versus patients with Chiari I malformations (F = 4.35; df = 1,15; P = .0001).

Note: SI indicates superior-inferior encoding; AP, anteroposterior encoding.

Fig 4. *E* and *F*, Velocity graphs of normal and Chiari tonsils (AP) and upper cords (AP). The signal intensity (proportional to velocity) is shown on the vertical axis, and the 16 data points (labeled X_1 to X_{16}, representing frames of the cardiac cycle) are on the horizontal axis. The graphs represent the mean values of the intensities at the different points in the cardiac cycle. One-standard-deviation error bars are shown. All *P* values represent significance levels with analyses of variance. In the anteroposterior series, negative intensities represent anteroposterior movement and positive intensities posteroanterior movement.

E, Medulla, anteroposterior encoding, healthy volunteers versus patients with Chiari I malformations (F = 7.10; *df* = 1,15; *P* = .0001). Note the opposite directional movements of the medulla in the healthy volunteers compared with the patients with Chiari I malformations.

F, Upper cord, anteroposterior encoding, healthy volunteers verusus patients with Chiari I malformations (F = 4.09; *df* = 1,15; *P* = .0001).

Note: AP indicates anteroposterior encoding.

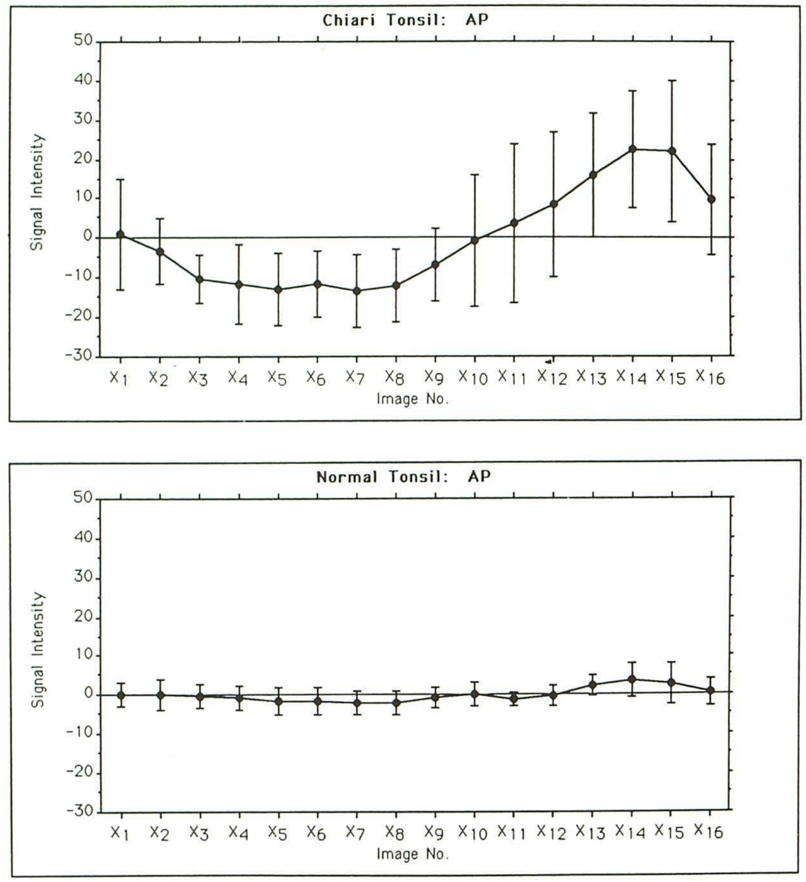

E

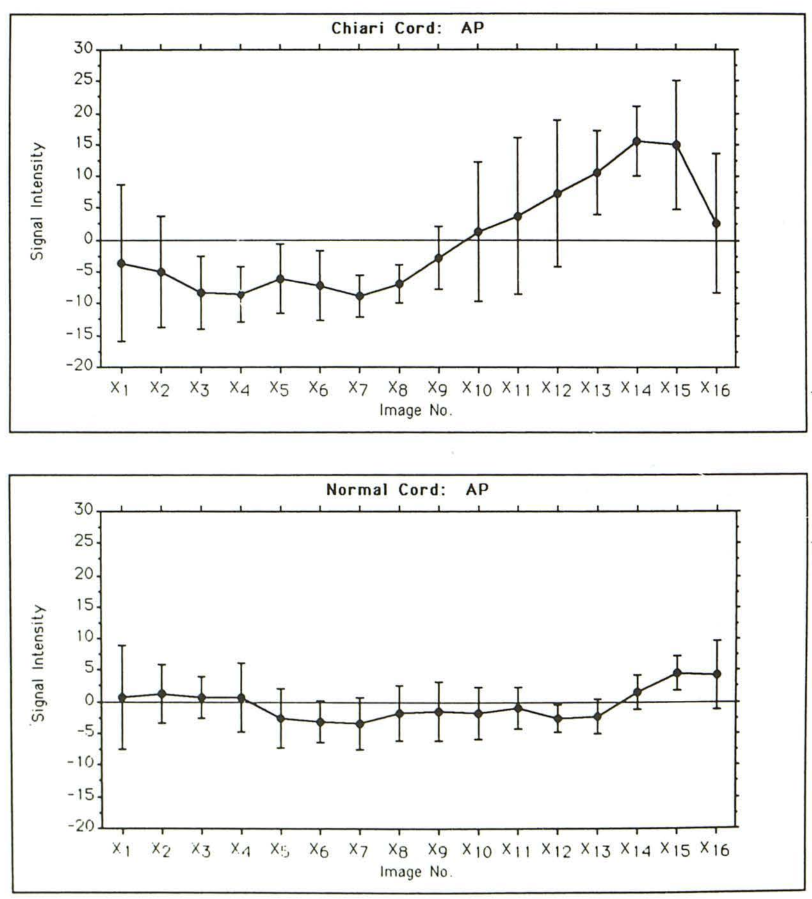

F

cerebellar tonsil occurred simultaneously with, and therefore was thought to account for, the caudal motion of the CSF in the cervical subarachnoid space. Poncelet et al demonstrated a lateral velocity component at the level of the thalami and third ventricle exceeding in magnitude an additional caudal velocity component of the central brain structures (12).

With this recent interest in the use of phase imaging to demonstrate brain motion and CSF flow, we set out to investigate the CSF dynamics in patients with Chiari I malformations. Phase-imaging methods, when applied to CSF and brain velocity studies, are hampered by low spatial resolution and destructive interference of spin phases (intravoxel incoherent motion), which can reduce the magnitude of the measured velocity greatly (13). Our data also may be suspect because of the relatively poor signal-to-noise values obtained with the selected velocity encoding of 5 cm/s. (Recently we modified the original sequences so that velocity encodings of 2 cm/s could be obtained. In one patient with Chiari I malformations not included in this study and scanned with velocities of 2, 5, and 7 cm/s, the signal intensity-versus-time curves of the medulla, tonsils, and upper cord were identical at all three velocities.) In the present study, to compensate for possible errors caused by gradient-induced currents, the average of the intensities at given regions of interest were subtracted from the measured values, but other than this, no further compensations were made.

Although we could not distinguish CSF flow through the valleculae from the adjacent brain movement in the patients with Chiari I malformations, in all probability obstruction of flow through the valleculae was present as has been previously described (4). Because hydrocephalus was not present, presumably normal flow occurred through the foramina of Luschka.

We are unsure of the significance of the increased velocities of the tonsils in the patients with Chiari I malformations over the volunteers. Du Boulay in 1974, using cine imaging after the instillation of Myodil (Pantopaque) into the subarachnoid space for myelography, also noticed increased downward velocities of the tonsils in 8 of 84 patients with Chiari I malformations (14). Enzmann and Pelc reported that the peak velocities of the tonsils in healthy subjects were approximately four times that of other brain structures. We, however, observed that the tonsillar velocities were 10 times that of control subjects and furthermore were associated with posterior excessive movement (compared with the normal anterior movement) of the medullae, resulting in systolic clockwise movement (as viewed from the left side) of the tonsils, upper cervical cords, and medullae in the patients with Chiari I malformations.

Before we can use our data clinically to separate nonsurgical patients from surgical patients or to relate the information to symptoms, the observations need to be explained. The increased velocities of the tonsils may be the result of the systolic pulse waves being delivered to a structure (the tonsil) without the normal surrounding cushioning CSF, resulting in an impact of the tonsil into the confined foramen magnum and a subsequent caudocraniad and posteroanterior recoil of the medulla. Another theory is that increased velocity of the tonsils is caused by a yet-unexplained mechanism that could be the cause of the malformation. A further theory would suggest that a Bernoulli effect caused by crowding of the tonsils into the foramen magnum causes an increased velocity of the tonsils. Finally, it is conceivable that the increased velocities are not unique to the Chiari I malformation but occur with any posterior-fossa mass.

The long-term and clinicopathologic effects of the increased velocities in the Chiari I malformation are uncertain. The commonly accepted practice for treating symptomatic patients with Chiari I malformations is suboccipital craniectomy and upper cervical laminectomy (1, 15). After this procedure many patients are benefited, although a significant proportion might be expected to relapse within 2 to 3 years. Headaches disappeared in four patients; in one patient the ataxia completely resolved; in another it improved; and in a third patient the scoliosis progressed after surgery. Five of the patients in the present study had velocity studies both before and up to 3.5 months after surgery. There was no change in the degree of tonsillar herniation as assessed on spin-echo images, and the postoperative flow studies demonstrated no change in the CSF flow patterns (although in three patients the valleculae became clearly distinguishable after surgery). In four of the five patients a decrease in the peak systolic velocities of the tonsils was seen, but not to normal values. We have not had sufficient follow-up time to comment about the long-term and clinicopathologic effects of the increased velocities in patients with Chiari I malformations, or to determine criteria for the selection of patients who may benefit from surgery. A larger study investigating flow studies and brain movement studies in patients with Chiari I malformations studied before and after surgery with a longer follow-up period is currently underway.

MR phase imaging provides a new radiologic method for imaging brain and CSF movement and velocity. The applications of this new technology have not as yet been fully realized. An immediate application would be in the study of lesions that could impede CSF flow at the foramen magnum such as the Chiari I malformation. Information gathered from these studies conceivably could be used to select patients who may or may not benefit from decompressive procedures and also to assess the benefits of surgery. In this study we found increased caudal and anterior velocities of the tonsils simultaneous with abnormal posterior velocities of the medullae. Preliminary data suggest that the tonsillar velocities may decrease after surgery. Theories are offered to explain the hypervelocities of the tonsils. We cannot as yet incorporate the velocity information in clinical treatment decisions. Long-term follow-up studies may be helpful.

Addendum

To assess the validity of the weighted-phase images we assessed the regions of interest in the medullae of all the volunteers and the patients in the magnitude images, and we found that the variation in regions of interest is minimal through the cardiac cycle, so a plot of the weighted-phase regions of interest for a given patient is still proportional to velocity. Compensation for the magnitude images in our summed data showed a slight (about 10%) reduction in the standard deviations.

References

1. Paul KS, Lye RH, Strang FA, Dutton J. Arnold-Chiari malformation: review of 71 cases. *J Neurosurg* 1983;58:183–187
2. DelaPaz RL, Brady TJ, Buanano FS, et al. Nuclear magnetic resonance (NMR) imaging of Arnold-Chiari Type I malformation with hydromyelia. *J Comput Assist Tomogr* 1983;7:126–129
3. Wolpert SM, Anderson M, Scott RM, Kwan ESK, Runge VM. Chiari II malformation: MR imaging evaluation. *AJNR Am J Neuroradiol* 1987;8:783–792
4. Quencer RM, Donovan Post M, Hinks RS. Cine MR in the evaluation of normal and abnormal flow: intracranial and intraspinal studies. *Neuroradiology* 1990;32:371–391
5. Levy LM, Di Chiro G, McCullough DC, Dwyer AJ, Johnson DL, Yang SSL. Fixed spinal cord: diagnosis with MR imaging. *Radiology* 1988;169:773–778
6. Feinberg DA, Mark AS. Human brain motion and cerebrospinal fluid circulation demonstrated with MR velocity imaging. *Radiology* 1987;163:793–799
7. Pelc NJ, Herfkens RJ, Shimakaxa A, Enzmann DR. Phase contrast cine magnetic resonance imaging. *Magn Reson Q* 1991;7:229–254
8. Enzmann DR, Pelc NJ. Brain motion: measurement with phase-contrast MR imaging. *Radiology* 1992;185:653–660
9. Chiari H. Uber veranderungen des Kleinhirns infolge von Hydrocephalie des Grosshirns. *Dtsch Med Wochenschr* 1891;17:1172–1175
10. Elster AD, Chen MYM. Chiari I Malformations: clinical and radiological reappraisal. *Radiology* 1992;183:347–353
11. Barkovich AJ, Wippold FJ, Sherman JL, Citrin CM. Significance of cerebellar tonsillar position on MR. *AJNR Am J Neuroradiol* 1986;7:795–799
12. Poncelet BP, Wedeen VJ, Weisskoff RM, Cohen MS. Brain parenchym motion: measurement with cine echo-planar MR imaging. *Radiology* 1992;185:645–651
13. Feinberg DA. Modern concepts of brain motion and cerebrospinal fluid flow. *Radiology* 1992;185:630–632
14. du Boulay G, Shah SH, Currie JC, Logue V. The mechanism of hydromyelia in Chiari type I malformations. *Br J Radiol* 1974;47:579–587
15. Oakes WJ. Chiari malformations, hydromyelia, syringomyelia. In: Wilkins RH, Rengachary S, eds. *Neurosurgery*. Vol 3. New York: McGraw-Hill, 1985;2102–2124
16. Oldfield EH, Muraszko K, Shawker TH, Patronas NJ. Pathophysiology of Syringomyelia associated with Chiari I malformation of the cerebellar tonsils. *J Neurosurg* 1994;80:3–15

Since acceptance of this manuscript a report (16) has appeared in which intraoperative ultrasonography demonstrated abrupt downward movement of the cerebellar tonsils during systole in patients with the Chiari I malformation.